

UC Berkeley

UC Berkeley Previously Published Works

Title

Focused and defocused retinal images with Bessel and axicon pupil functions.

Permalink

<https://escholarship.org/uc/item/0q524264>

Journal

Journal of the Optical Society of America. A, Optics, image science, and vision, 37(1)

ISSN

1084-7529

Author

Westheimer, Gerald

Publication Date

2020

DOI

10.1364/josaa.37.000108

Peer reviewed

Focused and defocused retinal images with Bessel and Axicon pupil functions

GERALD WESTHEIMER¹

¹ Division of Neurobiology
University of California at Berkeley,
Berkeley, CA. 94720, USA
gwestheimer@berkeley.edu

ABSTRACT. Retinal image light distributions in a standard optical model of a diffraction-limited eye with round pupils are presented for several patterns of amplitude and phase modulation of the light admitted into the eye. Of special interest are circularly symmetrical configurations of truncated Bessel amplitude transmission functions, and of light subjected to axicon deviation. It is shown by several examples that this kind of beam shaping allows generation of retinal imagery which can be more robust to defocus while maintaining minimal image degradation and it points to situations of two separate zones simultaneously in sharp focus, several diopters apart. © 2020 Optical Society of America

OCIS Codes 330.4460, 330.4595, 330.7333

1. INTRODUCTION

The ability to sophisticatedly modulate amplitude and phase relationship across the pupil of the light entering the eye is advancing so well that it is fruitful to explore in a general way how the retinal light distribution is affected by various light patterns in the pupil plane. Phase changes to null out aberrations are now a staple in adaptive optics but the promise of amplitude modulation [1] has remained largely unfulfilled. Here attention will be given to light entering the eye with cross-sectional profiles of Bessel functions and axicons.

Of interest is the irradiation on the retinal surface when the light entering the eye has been conditioned by various programs of circularly symmetrical complex amplitude pupil transmission functions. Because the propagation of beams in the image space is then not conventional, the effect of defocus will need specific investigation. In a beginning survey intended to gauge the potential for generating retinal light stimuli in experimental visual science and clinical practice, the study concentrates on aberration-free eyes with a moderate pupil diameter.

1.1 Bessel Beams

In the strict interpretation, a Bessel beam is the situation in which the cross-sectional amplitude profile of a plane wave is that of a Bessel function, usually of the first kind and zero order, $U(r) = J_0(q \cdot r)$, r being the radial distance from the axis and q a parameter, in reciprocal units of length (Fig. 1). The function reaches its first several zeros for $q \cdot r = 2.3, 5.6, 8.7, 11.8, \dots$. If such a beam is intercepted by a light-detecting surface, for example, a sheet of photographic film, a high-resolution photodetector array or the retina, an irradiation pattern will be measured corresponding to the light intensity $I(q \cdot r) = U(q \cdot r) \cdot U'(q \cdot r)$ and no longer reveal the phase of the actual electro-magnetic disturbance, which in the Bessel configuration has a 180 degree shift at each zero crossing. If there is a real opacity with such a pattern in the pupil, just the intensity is modulated by $I(q \cdot r)$, the equi-phase surface remaining that of a plane. The distinction between $U(q \cdot r)$ and $I(q \cdot r)$ matters when the further evolution of the beam is studied.

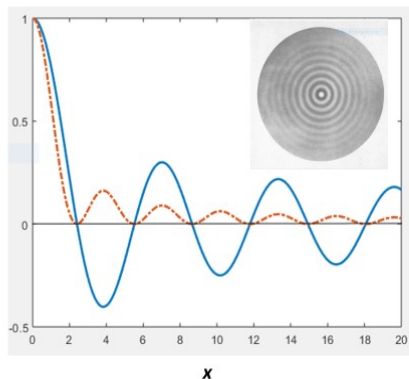


Figure 1. Cross-sectional profile of Bessel beam $J_0(r)$, showing the first few lobes. Solid line: amplitude of a true Bessel beam. Dotted line: transmissivity of an opacity conforming to a Bessel function with the same parameter. The first few zeros occur at 2.4, 5.5, 8.6, 11.8 ... Insert: Face-on appearance of a Bessel intensity function.

1.2 Axicon

An axicon [2] is a circularly symmetric centered conical optical element with apical angle χ radians, made of material of refractive index n . It imposes on all incident rays a coplanar deviation towards (or away from) the axis by an angle $\delta = (n-1) \cdot \chi$ radians (Fig 2). That means that an incident plane wave normal to the axis is converted into a conical sheaf of plane waves (equal-phase surfaces), each point on the incident plane wave having its phase shifted, circularly symmetrically, by $2\pi \cdot \delta \cdot r/\lambda$ radians, where r , the radial distance from the axis, and λ , the light's wavelength, are in the same units of length.

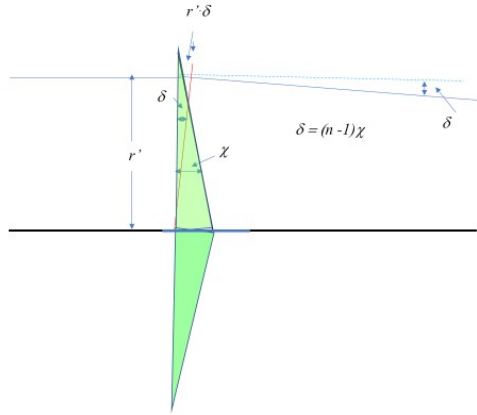


Figure 2. Rays as deviated by a purely prismatic axicon with apical angle χ . All rays are deviated towards (or away from) the axis through an angle $\delta = (n-1) \cdot \chi$. At a distance r' from the axis, the optical path between the incident plane and the point of interception by the receiving plane is changed by a phase factor $2\pi \delta \cdot r'/\lambda$.

2. Theoretical Formulation

Of central interest is the light distribution in the retinal image as it is generated by the eye's optics and defined by the amplitude and phase of the electromagnetic disturbance in the plane of the entrance pupil. The computational strategy [3] proceeds from the pupil function $A(r_p)$ to the retinal intensity distribution in the image of a point object, the point-spread function $I(r_r)$, via circular Fourier (Hankel) transformation followed by multiplication with the complex conjugate (squaring). By concentrating the analysis on the changes when the stimulating beam is modified in a given eye, some differences in constants of proportionality need not be addressed.

A convenient initial setting is that of a standard 60 diopter eye with a round entrance pupil of radius $r_{p,r}$, monochromatic light of wavelength λ in air, and image light properties referred back to the object space. Retinal image distances are expressed in object-sided visual angles, and defocus ΔF in diopters. This situation would pertain immediately to wavefront-corrected eyes. Phase deviations in the pupil plane, originally computed as distances in air Δs , are converted to φ , the phase angle of the electromagnetic disturbance in radians, by the formula $\varphi = \Delta s \cdot k$, where $k = 2\pi/\lambda$. The pupil transmission function takes on the form

$$(1) \quad A(r) \cdot e^{-i\varphi(r)}$$

A specific instance of a phase effect is defocus [4], when the center of the wavefront emerging from the eye's exit pupil no longer coincides with the retina but has shifted to a position corresponding to ΔF diopters defocus. In the pupil the wavefront now deviates by $\beta \cdot \Delta F \cdot r_p^2$, which makes the phase factor in equation (1) $\exp(-i \cdot k \cdot \beta \cdot \Delta F \cdot r_p^2)$. For the standard ametropia conditions considered here, the constant β evaluates to $0.125 \cdot 10^{-3}$ when r is in millimeters and ΔF in diopters.

3. Specific Pupil Functions

3.1 Bessel Beams

Consider the case of the entering beams whose cross-sectional profile is a Bessel function centered on the eye's optical axis. This means that the factor $A(r_p')$ has become $J_0(q \cdot r_p')$ or $\sqrt{(J_0(q \cdot r_p'))^2}$ depending on whether one is dealing with a true Bessel beam or an opacity with the ring pattern of a Bessel beam. The Bessel function's parameter q controls its tightness and hence the number of lobes admitted into the eye. Applied here to a pupil radius of r_p in $J_0(q \cdot r_p')$ it assumes the values $2.40/r_p$, $5.52/r_p$, $8.65/r_p$, $11.79/r_p$ depending on whether the pupil should contain just the central lobe of the Bessel function or also encompass the next successive second, third, fourth .. zeros. Thus, for example, a pupil of radius 2 mm will admit the central lobe and the first surrounding ring of a Bessel beam with parameter $q = 2.76$. For a true Bessel beam, this surrounding zone will have a negative amplitude of 0.4 of the central peak whereas in a Bessel opacity there is an intensity reduction of 0.16 for the first surround ring.

This analysis is now applied to the standard eye with attention to the quality of the retinal image, by computing the retinal irradiance along a retinal meridian, characterizing a circularly symmetrical point-spread function. Of most importance is how complete the Bessel function is, i.e., how many of its multiple lobes are admitted into the pupil. If it is substantially complete, then the retinal image will be a sharply focused ring of light, for that is the Fourier transform of a Bessel function of zero order. Here the other end of the problem is investigated because the interesting and potentially useful, from the optometric standpoint, situations arise when the pupil aperture admits a Bessel beam truncated to just the beginning few lobes.

To illustrate the effects that can be achieved, the results of the computation for three paradigmatic conditions are presented in Fig. 3: a pupil 2 mm in radius, light of wavelength 0.55 nm, Bessel aperture functions with parameter $q = 0$, 1.38 and 5.6, and retinal irradiance in the range 0 - 3 arcmins from the axis and spanning a defocus from +2.5 to -2.5D. The figure features in each of its three panels: top, the radial pupil amplitude profile and below, a three-dimensional graph of the retinal irradiance in a cross-section of the point-spread function in a range of image planes between 2.5 Diopters hyperopic and 2.5 D myopic defocus, for the null condition of uniform incident plane wavefront.(Fig. 3 left) and for truncation values of the Bessel function, selected to reveal two particularly notable regimens. One of these (Fig. 3, middle) provides enhanced depth of focus around the geometrical focus with minimal widening of the point-spread function, the other (Fig. 3, right) a dual focus situation in which sharp point-spread functions are generated in two separate zones of focus, several diopters apart, each with its own depth of focus which resembles that in full-pupil imagery. They are merely examples of specific truncations of canonical Bessel functions. It is of course possible to refine these retinal images in order to mitigate unwanted components by exploring more sophisticated complex pupil transmission functions than just those based on the Bessel form.

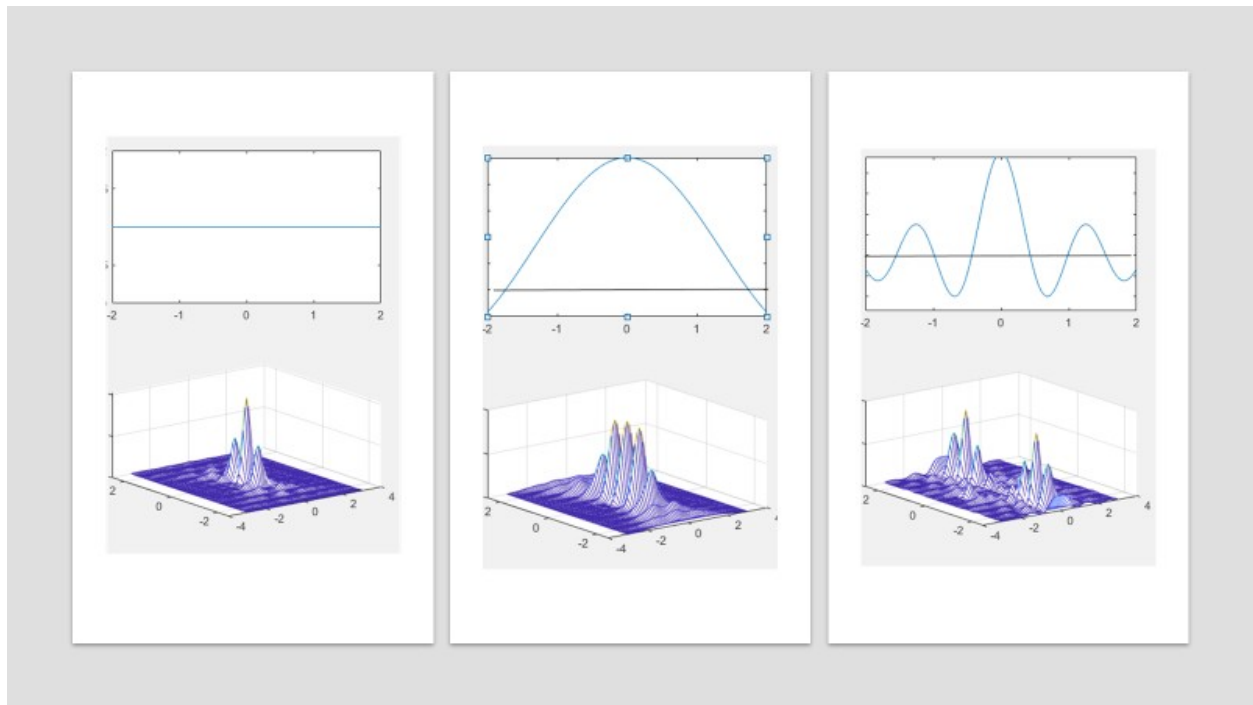


Fig. 3. Retinal Imagery with Bessel beam illumination. In each panel, top: amplitude distribution radially across the eye's 2mm-radius entrance pupil, (below) cross-section of the retinal illuminance through the center of the circularly symmetrical point-spread function in a range of image planes in $\frac{1}{2}$ Diopter steps from 2.5D myopic to 2.5 D. hyperopic defocus.

From left to right: (Left) Normal viewing, full pupil transmission; (Middle) Bessel amplitude pupil transmission, truncated to admit a little more than only the central lobe; (Right) Bessel amplitude pupil transmission, admitting to the third zero. Compared with normal viewing, Bessel function amplitude modulation of pupil transmission can produce, depending on the degree of truncation, increased depth of focus (middle), or two sharp zones of good quality image, several diopters apart (right).

3.2 Axicon

When the axicon's and eye's axes coincide, there is circular symmetry, and it suffices to consider axicon beam imagery in a single meridian. The relevant parameter is the angle δ through which the axicon deviates each ray in the beam – towards or away from the axis -- in its meridional plane. The regime considered here is the one in which an axicon-like effect is incorporated in an intra-ocular or contact lens correction, in or near the eye's entrance pupil, partitioning the pupil aperture in a circularly symmetrical fashion. It introduces a phase change proportional to the radial distance from the pupil center. When the deviating angle of the axicon is small, the effect on the retinal image simulates that of a

change in focus (Fig. 4). In general, as the optimum focus plane shift away from the geometrical center of the spherical wavefront with increases in small-angle axicon power, the depth of focus increases with a modest diminution of the Strehl ratio.

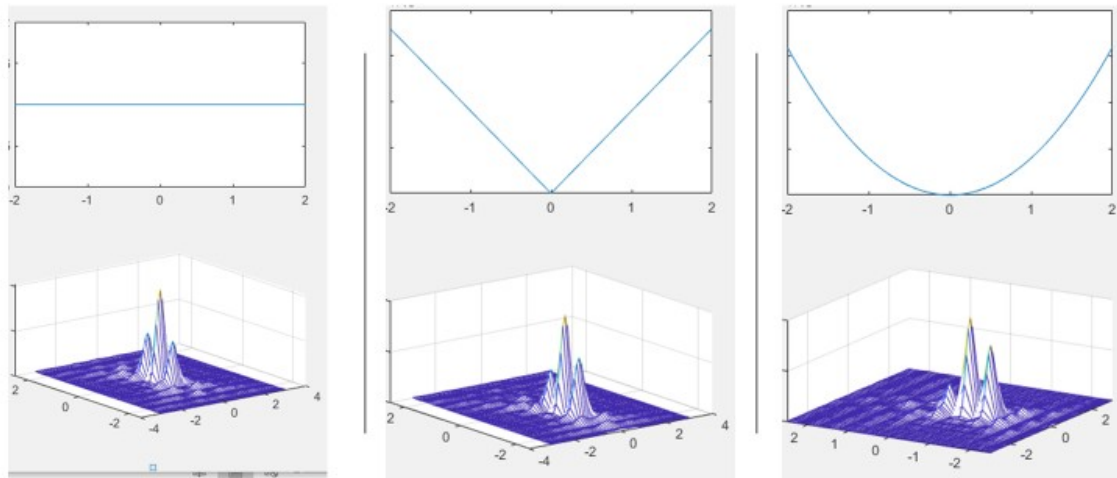


Fig. 4. Retinal image with small-angle axicon pupil modulation.

(Top) Path difference phase deviations from sphericity of the wavefront admitted into the eye's pupil (phase deviations) and (bottom) cross-section of retinal illuminance through the center of the point-spread function in a range of image planes in $\frac{1}{2}$ Diopter steps from 2.5D myopic to 2.5 D. hyperopic defocus in three conditions. Left: Normal viewing, in focus, Middle with a coaxial axicon, deviating angle 0.3 milliradians, in or near the eye's entrance pupil, phase increases linearly with radial distance in the pupil. (Right) normal viewing with 1D defocus, when there is a quadratic phase deviation of the wavefront. Comparison with equivalent panels in Fig. 3 shows that the effect of a small-angle axicon in or near the pupil is akin to changing focus..

For axicons with larger values angles of deviation, the retinal image becomes a ring (Fig. 5): opposite halves of each meridional sheet of rays in their passage through the pupil are deviated through equal but opposite angles and come to a focus on the retina at the off-axis distance determined by the axicon's deviating angle. This is useful for reaching far peripheral regions of the retina.

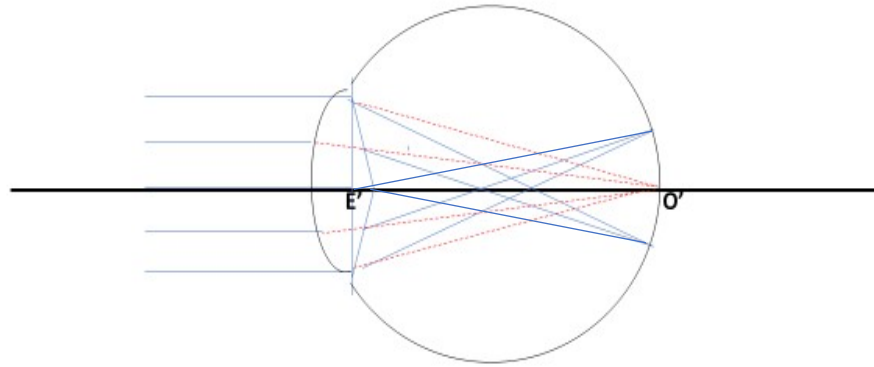


Fig. 5. An axicon with larger deviating angle placed in or near the eye's entrance pupil E' deviates meridional sheets of rays away from Gaussian focus O' to peripheral locations, forming a ring image. Solid lines: axicon imagery, dotted lines: normal path of light from lens to retina.

The situation changes materially when the axicon is moved away from the eye; then, instead of the axicon's beams partitioning the pupil, the entire pupil is filled simultaneously by overlapping beams from all sectors around the clock originating on the separate sides of the axis (Fig. 6, position P .) With appropriate disposition of the element relative to the eye, the disturbance in the pupil plane would be a Bessel or quasi-Bessel beam [5,6], and can give rise to concentric ring retinal image patterns. This procedure has been pioneered [7] and implemented to control fixation [8].

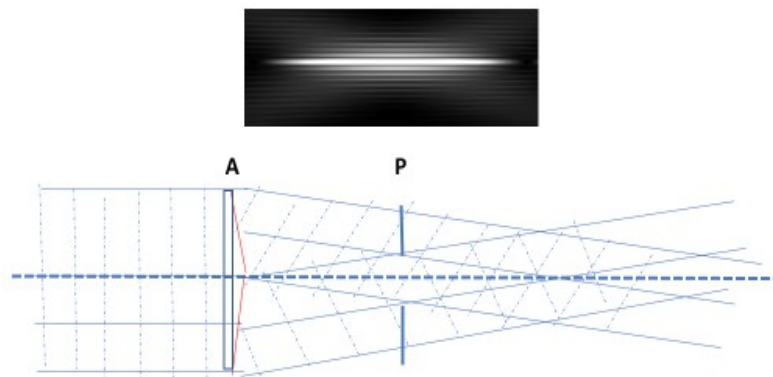


Fig.6. Rays from a parallel beam traced through a purely prismatic axicon A . When the pupil of a viewing eye is placed at P , deviated beams from all half-meridians around the clock fill the pupil, all participating in the generation of the interference pattern that is admitted into the eye's pupil. There is a zone in the axicon's image space in which the cross-sectional light distribution is that of a Bessel or quasi-Bessel beam. [6].

4. Discussion

To illustrate how manipulations of the complex amplitude of the wave-front admitted into the pupil of an eye can achieve retinal image light distributions with specific properties,

quantitative relations were obtained for representative values of the pupil diameter and wavelength, 4mm and 0.55nm respectively. They would apply with suitable scale changes when these numbers are different. Among the specific situation of circularly symmetrical pupil patterns, concentric with the eye's optical axis, the simplest is the axicon, with no amplitude attenuation and a phase that changes linearly with radial distance from the axis. Mathematically the next level is a quadratic phase change which is the time-honored spherical power in the eye's refraction. Bessel functions, the two-dimensional rotational analogues of one-dimensional sinusoids, are obvious candidates for a further level of sophistication, but consideration need not stop with them, nor does it preclude combination of a variety of circularly symmetrical patterns. Altogether, the richer potential of other phase manipulations remains to be explored.

4. 1 Real eyes versus their diffraction-limited models.

The formulation here, viz., the diffraction limit when monochromatic radiation is incident on an aberration-free model standard eye, represents the minimum departure from pure geometrical optics that can be considered with some semblance of generality. In real life situations it is conflated with a number of additional factors, the degree of whose dilution of the generality of the current model will have to be evaluated as the concepts are translated into practice.

Ordinarily, light is not monochromatic, but it is within the purview of this approach to extend computations over the wavelength spectrum and integrate the result based on the applicable luminosity curve. This is a problem, and has a solution, shared with all purely optical analyses, as are, of course, a whole host of factors concerned with transmission in the ocular media and retinal light transduction. More apropos is the fact that real eyes suffer from aberrations and defects, increasingly so with increases in pupil diameter. Moreover, pupillary and accommodative instability abound. The combination of these factors prevents the direct application of the current computational results to any specific human visual situation except those in which deviations from sphericity of the wavefront converging on the retina have been nulled out by adaptive optics. But the broad outlines are likely to still hold when the calculations start with the actual optical transfer function of an eye in place of the ideal one. For example, according to Artal the transfer function of his eye with a 4 mm diameter pupil approximates that of a slightly defocused diffraction-limited one with a 2mm pupil [9]. When the Bessel and axicon pupil modulations considered here are introduced in such a situation, the described retinal image feature changes still hold. Fig. 7 illustrates how similar the in-focus point-spread functions in the horizontal meridian of this real eye with plain illumination is to that in the 1.5 D defocus plane with a suitably truncated Bessel function pupil transmission.

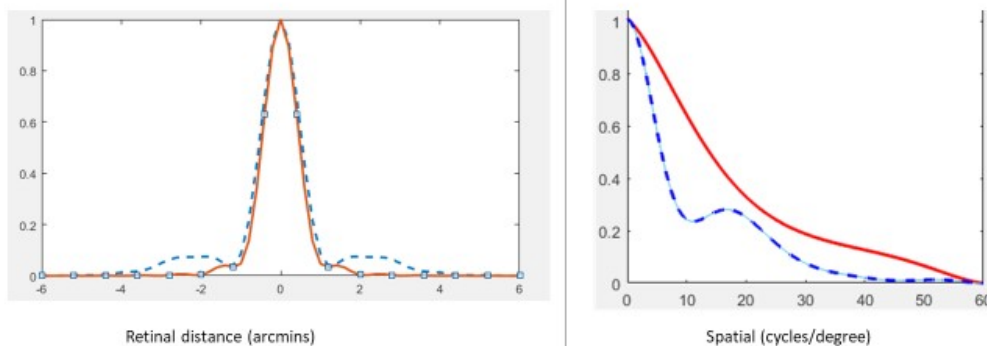


Fig. 7. Retinal image in an actual eye (data from Artal [9]). Left: cross-section of point-spread function through its center; right optical transfer function. Two conditions. Solid lines, normal in-focus viewing, dashed lines, with in 1.5 Diopter defocus with truncated Bessel function pupil modulation (normalized). The figure shows the expected effect of suitable pupil transmission modulation functions on ocular imagery in a real eye.

Human vision is, of course, not just ocular optical imaging. Yet that step is necessarily always involved and, to the extent that it can be known and controlled, contributes to the depth of our understanding and ability to provide diagnosis and therapy of infirmities and enhance the capabilities of vision.

4. 2 Measures of Image Quality and Degradation

Right from the outset, their provision of augmented depth of focus had been hailed as an advantage of Bessel beams [10]. Lambert et al. have recognized this and understood it to be a consideration that enters in experiments to improve fixation quality [7]. And the diminution of utilized pupil area suggests a connection with the phenomenon of apodization and the associated changes in image light spread [11]. But depth of focus is a somewhat broad concept. In the study of the visual ability for spatial discrimination, the optical fundament is the retinal light spread for a monochromatic point source; all further considerations of the spatial properties of visual stimuli can be reduced to it. Though it contains the full information, it has more details than can often be assimilated. If a single-valued measure is sought, the Strehl ratio [12] is sometimes quoted. The width-at-half-height is perhaps somewhat more informative but the display in some of the figures in this paper make it apparent that for out-of-focus states it is often ambiguous and multi-valued. The optical transfer function, in the Fourier domain, remains a popular descriptor and is particularly useful when vision is embedded in a sequence of other optical and electronic operations. But a graph of the response to sinusoidal gratings as a function of spatial frequency fails to serve at an intuitive level as an unmediated indicator of image quality, especially where there are phase components. In its immediate, intuitive appeal from both the perspective of visual perception, and of conclusion from inspection of a graphical representation, a better candidate would seem to be the step function response, i.e., light distribution in the image of a straight edge. In the context of the present calculations, it is

computed via the Optical Transfer Function in systems with complex-amplitude pupil transmission by following the sequence [132,14]: pupil complex amplitude \rightarrow autocorrelation \rightarrow cosine transformation, leading to line-spread intensity function \rightarrow integration. If a single-valued measure is desired, it might be the reciprocal of the ogive's slope in its middle: the sharper the image the smaller that value.

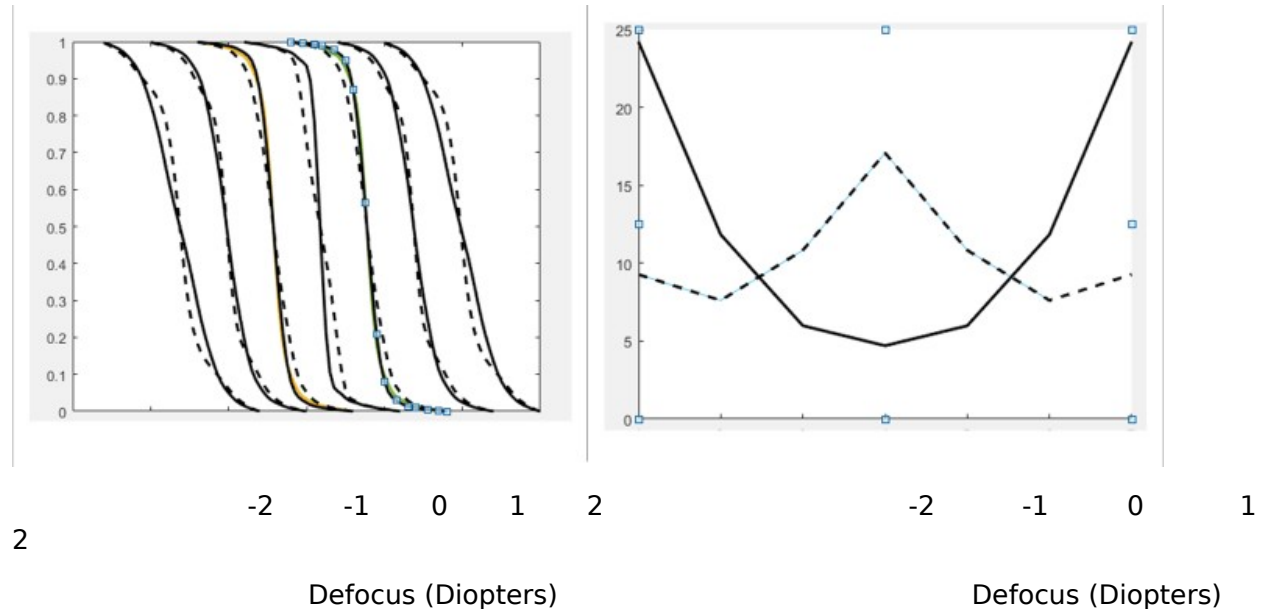


Fig. 8 Left: Light distributions in the retinal image of an edge in focus (middle of the seven ogives) and in three equally-spaced states of defocus both in the myopic and hyperopic directions. Solid lines, normal viewing – plane wavefront, dashed lines with a pupil admittance of the form of a truncated Bessel beam. The latter condition gives an image in two separate states of defocus that is almost as sharp as that in the in-focus condition with normal viewing.

Right: A measure of image degradation – the reciprocal of the edge gradient at the middle of the ogive light distribution of a sharp target edge as seen on the left of the figure – as a function of state of focus for both normal viewing (solid curve) and Bessel beam imagery (dashed curve). The graph tellingly illustrates the dual-focus property of this type of Bessel beam.

An example of the approach can be seen in Fig. 8. On the left panel, light spreads in the diffraction-limited images of a sharp geometrical target edge are drawn for in-focus imagery (center ogive) and three equally-spaced out-of-focus states on each of the myopic and hyperopic sides. The solid curves refer to the normal case of a uniform open pupil admittance, the dashed lines to the case in which the eye's pupil admittance function is a Bessel beam truncated before the second zero crossing. The right panel of the figure depicts a measure of the image degradation, specifically the reciprocal value of the edge gradients at their midpoint, as a function of defocus for the two viewing conditions. The latter graph allows a good grasp of the concept of the dual focus state generated when the pupil aperture has been conditioned to a certain kind of Bessel beam: There are now two zones, several diopters' viewing distance apart, each with good imagery and with commendable depth of focus. Object positions lying between them are imaged on the retina with prominent blur. A presbyopic or aphakic wearer of such an optometric correction would encounter a substantially different experience than with a conventional multifocal spectacle correction where in a given gaze direction there is a single zone of clear focus and focus changes are accomplished by gaze shifts. With a "Bessel lens" along each line of sight there are *two* focus zones in which vision is sharp; in their interval and beyond them, there is blur.

4.3 Clinical and Research Application

The examples presented in this study draw attention to the wide potential of customizing retinal images through sophisticated amplitude- and phase conditioning of the wavefront admitted into the eye's pupil. The manner and possible scope of their actual practical application, as seen from the current perspective, merit consideration.

First, to be of practical utility, there is need for physical implementation. When part of equipment in bench setups or in more elaborate ophthalmic instrumentation, wavefront modification by means of spatial light modulators would be the method of choice. Reflecting phase modulators are routine components in adaptive optics, but the transmissive type, allowing both amplitude and phase modulation, are already beginning to be sufficient in pixel count, compactness and precision of control to be put into operation in vision research and for clinical diagnostic purposes. In addition, the study points to a future in which intra-ocular or contact lenses are designed and fitted incorporating wavefront modifications that lead to retinal image patterns with specific desirable properties in individual patients. They would need to have complex surfaces, but a future can be foreseen when they might be constructed of materials where optical phase is controlled by localized refractive properties rather than physical path length.

This study has concentrated on beam shaping by just truncating Bessel beams of the first kind and zero order. Even then, a previously known as well as a very desirable new property have emerged. Depth of focus [15] is an important issue for the large segment of the population that is presbyopic or aphakic following surgery, and therefore cannot rely on the eye's intrinsic accommodation apparatus. Bessel-function wavefront patterns clearly take their place among methods of increasing depth of focus, perhaps in conjunction with further deviations from sphericity. That suitable truncation of Bessel beams can generate multifocal situations, Fig. 3, right, and Fig. 8, above, seems not to have been pointed out before. The situation of two zones of sharp imagery along a single line of sight, several diopters apart, each with its own respectable depth of focus, would be implemented in practice by adding a spherical component that shifts the object location of one of the zones to infinity and the other to a close-up distance. The virtue of this arrangement is that, as distinct from the methods in which depth of focus is enhanced at the expense of sharp imagery, there is only very little degradation in the two good focus locations.

Nothing said so far precludes further refinement of retinal image properties by yet more sophisticated wavefront shaping, once it is accepted to extend the concept of refractive correction beyond standard spherical and toric surfaces and begin constructing individualized contact or intraocular optics. This would depend on these two facets of implementation: (1) Advances in material science and practical clinical techniques, and (2) procedures, including empirical ones involving trial and error (i.e., AI) on patients' eyes, to determine optimum wavefront amplitude and phase parameters for the desired outcome.

Funding

There were no external funding sources for this study.

Disclosures

The author reports no conflict of interest.

References

1. J. Liang and G. Westheimer, "Method for measuring visual resolution at the retinal level", *Opt Soc Am A* **10** (8), 1691-1696 (1993).
2. J. H. McLeod, "The Axicon: A New Type of Optical Element", *J. opt. soc. Am.* **44**, 592-597 (1954).
3. G. C. Steward, *The Symmetrical Optical System*. (University Press, Cambridge, 1928).
4. H. H. Hopkins, "The frequency response of a defocused optical system", *Proc. roy. Soc. (Lond.) A* **231** (91-103) (1955).
5. D. McGloin and K. Dholakia, "Bessel beams: diffraction in a new light", *Contemporary Physics* **46** (1), 15-28 (2005).
6. T. Čižmár and K. Dholakia, "Tunable Bessel light modes: engineering the axial propagation", *Opt. Express* **17** (18), 15558-15570 (2009).
7. A. J. Lambert, E. M. Daly and J. C. Dainty, "Improved fixation quality provided by a Bessel beacon in an adaptive optics system", *Ophthalmic Physiol Opt* **33**, 403-411 (2013).
8. D. Bhattarai, M. Suheimat, A. J. Lambert and D. A. Atchison, "Fixation stability with Bessel beams", *Optom Vis. Sci* **96**, 95-102 (2019).
9. P. Artal, "Calculations of two-dimensional foveal retinal images in real eyes", *J. opt. soc. Am. A* **7**, 1374-1381 (1990).
10. G. Bickel, G. Häusler and M. Maul, "Triangulation with expanded range of depth", *Optical Engineering* **24** (6), 975-978 (1985).
11. B. Dossier, "Recherches sur l'apodisation des images optiques", *Revue d'Optique* **33**, 57-267 (1954).
12. K. Strehl, "Aplanatische und fehlerhaft Abbildung im Fernrohr", *Zeitschrift für Instrumentenkunde* **15**, 362-370 (1895).
13. E. L. O'Neill, *Introduction to statistical optics*. (Addison-Wesley, Reading, Mass, 1963).
14. J. W. Goodman, *Introduction to Fourier Optics*. (McGraw-Hill, San Francisco, 1968).
15. N. Charman, in *Handbook of Optics*, edited by M. Bass (McGraw-Hill, New York, 2010), Vol. 3, pp. 1.1-1.65